I. INTRODUCTION

When UAV executes missions in the complex environment, it is required to be able to adapt to the environment and can automatically plan flyable path online under encountering obstacles. As the motion of the UAV's platform is high-speed in real time, the independent control system of platform must operate and compute in real time. As a result, lots of offline methods which are time-consuming and have large calculation quantity, such as some intelligent optimization algorithms[1], aren't applied directly.

Some scholars put forward that the curve can be applied to path planning directly, which is easy to trace, for example, Dubins curve is applied to multiple UAVs' path planning which Shanmugavel, M.,et al[2] propose. Dubins path is composed by segmental arc and straight line, and from the perspective of the theory of differential geometry, in order to get a smooth flight path, the first two derivative of the path exists at least, that is, the curvature of the curve is continuous. Dubins path is the curve of C_1 type, but not the curve of C_2 type. Literature [3] gives the method of obtaining the path of continuous curvature by Clothoids curve. And the curvature changes linearly along the path, but the length of the path is not easy to generate closed solution. K.G. Jolly[4] applies the Bezier curve to the mobile robot's path planning. Literature [5] plans the parafoil terminal guidance path using the Bezier curve. Literature [6] plans the three dimensional flight path for UAV by using the Bezier curve of seven order, which considers climbing angle, curvature, torsion and so on system performance constraints. At present, Pythagorean Hodograph (PH) curve is widely used in aircrafts' on-line path planning[7-10], and the planning path is a path of C_2 type which the curvature is continuous. In contrast to other curves, it has a lot of advantages. The overall curvature of the curve is small. The length, curvature and bending energy of the curve can be calculated in closed form. The position and direction of the start point and end point are directly used in boundary conditions. The length and curvature can be coordinated easily. The generation of PH curve can be based on the Bezier spline curve, so it also has the advantages of the Bezier curve. Among them, the quintic PH curve is the lowest order PH curve which contains inflection points. Inflection points make the flight path have better flexibility, and to plan flight path better.

The generation method of PH curve path is given in literature [7]. Considering the performance constraints, such as curvature constraint, torsion constraint and so on, the length of beginning and

dimensional reduction is used to the obstacle avoidance, and the path can be re-planned by giving the insertion point of obstacle avoidance.

II. DESCRIPTION OF 3-D ONLINE FLYABLE PATH PLANNING PROBLEM

a. Constraints and performance metrics of 3-D PH path planning

It is assumed that the starting position $p_s(x_s, y_s, z_s)$, starting angle (θ_s, ϕ_s), ending position $p_f(x_f, y_f, z_f)$ and ending angle (θ_f, ϕ_f) are known, that is, the positions and poses of starting and ending points are $pose_s(x_s, y_s, z_s, \theta_s, \phi_s)$ and $pose_f(x_f, y_f, z_f, \theta_f, \phi_f)$ respectively. Among them, θ is the climbing angle and ϕ is the head angle. The UAV path is defined as $r(t) = [x(t), y(t), z(t)]$, and its curvature and torsion are κ and τ respectively. The formula of path planning can be expressed as: $pose_s(x_s, y_s, z_s, \theta_s, \phi_s) \xrightarrow{r(t)} pose_f(x_f, y_f, z_f, \theta_f, \phi_f)$, the picture representation of this problem is shown in figure 1. When the UAV detects the obstacle, the path interruption point should be calculated, and the path will be re-planned between the interruption point and the ending point.

Figure 1. 3-D Path Planning

Planning path $r(t)$, the following constraints need to be satisfied,

(1) Curvature constraint

$$|\kappa(t)| \le \kappa_{\max} \qquad (1)$$

$\kappa_{\max}$ is the biggest curvature constraint of planning path.

$$J = \min(\lambda_1 \times s + \lambda_2 \times \bar{\kappa}_{\max} + \lambda_3 \times \bar{\tau}_{\max} + \lambda_4 \times \bar{\theta}_{\max})$$

The performance indicator J consider the constraints of curvature, torsion, climbing angle and the length of path comprehensively, which can make re-planning path satisfy the requirements of performance indicator and can quickly reach the goal.

b. Generation of three-dimensional PH path

The spatial polynomial curve $r(t) = x(t)i + y(t)j + z(t)k$ can be expressed by the method of quaternion, and it is PH curve only when $r(t)$ meets the following form,

$$\frac{dr(t)}{dt} = A(t)iA^*(t) \qquad (7)$$

Among them, $A(t)$ is the polynomial of quaternion, that is $A(t) = u(t) + v(t)i + p(t)j + q(t)k$.

In order to define spatial PH curve, to consider quadratic Bezier polynomial

$$A(t) = A_0(1-t)^2 + A_1 \bullet 2(1-t)t + A_2 t^2 \qquad (8)$$

Its coefficients of quaternion are:

$$A_r = u_r + v_r i + p_r j + q_r k$$

Among them, $r = 0,1,2.$

So the rate $\sigma(t)$ of planning path can be get,

$$\sigma(t) = u^2(t) + v^2(t) + p^2(t) + q^2(t) \qquad (9)$$

According to the equation (9), the length of path can be accurately calculated by using the formula (6).

The relationship of 6 control points $P_0 \sim P_5$, which the generation of three-dimensional PH curve needs, is given in literature [8].

$$P_1 = P_0 + \frac{1}{5} A_0 i A_0^* \qquad (10)$$

$$P_2 = P_1 + \frac{1}{10}\left(A_0 i A_1^* + A_1 i A_0^*\right) \qquad (11)$$

$$P_3 = P_2 + \frac{1}{30}\left(A_0 i A_2^* + 4A_1 i A_1^* + A_2 i A_0^*\right) \qquad (12)$$

$$P_4 = P_3 + \frac{1}{10}\left(A_1 i A_2^* + A_2^* i A_0^*\right) \qquad (13)$$

A_0 , A_1 and A_2 can be obtained from the starting point P_0 and ending point P_5 . The values of P_1, P_2, P_3 and P_4 can be calculated according to the formulas (10) - (14), and then put them into the formula:

$$r(t)=\begin{bmatrix}1 & t & t^2 & t^3 & t^4 & t^5\end{bmatrix}\begin{bmatrix}1 & 0 & 0 & 0 & 0 & 0\\ -5 & 5 & 0 & 0 & 0 & 0\\ 10 & -20 & 10 & 0 & 0 & 0\\ -10 & 30 & -30 & 10 & 0 & 0\\ 5 & -20 & 30 & -20 & 5 & 0\\ -1 & 5 & -10 & 10 & -5 & 1\end{bmatrix}\begin{bmatrix}P_0\\ P_1\\ P_2\\ P_3\\ P_4\\ P_5\end{bmatrix} \qquad (20)$$

That is, the PH curve can be solved.

c. Analysis of 3-d PH path planning

It can be seen, from the generating process of PH curve, that the generating path is determined by the coordinates of the starting and ending points (P_s, P_f) ,the tangents' direction angles $(\phi_s, \theta_\mathrm{s}, \phi_\mathrm{f}, \theta_\mathrm{f})$, the tangents' length $(\varepsilon_s, \varepsilon_f)$ and three free angles (ξ_0, ξ_1, ξ_2) .

$$dx_s = \varepsilon_s \cos\theta_s \cos\phi_s$$

$$dy_s = \varepsilon_s \cos\theta_s \sin\phi_s$$

$$dz_s = \varepsilon_s \sin\theta_s$$

$$\varepsilon_s = \sqrt{dx_s^2 + dy_s^2 + dz_s^2} \qquad (21)$$

$$dx_s = x_1 - x_0$$

$$dy_s = y_1 - y_0$$

$$dz_s = z_1 - z_0$$

$$dx_f = \varepsilon_f \cos\theta_f \cos\phi_f$$

$$dy_f = \varepsilon_f \cos\theta_f \sin\phi_f$$

$$dz_f = \varepsilon_f \sin\theta_f$$

$$\varepsilon_f = \sqrt{dx_f^2 + dy_f^2 + dz_f^2} \qquad (22)$$

$$dx_f = x_5 - x_4$$

$$dy_f = y_5 - y_4$$

$$dz_f = z_5 - z_4$$

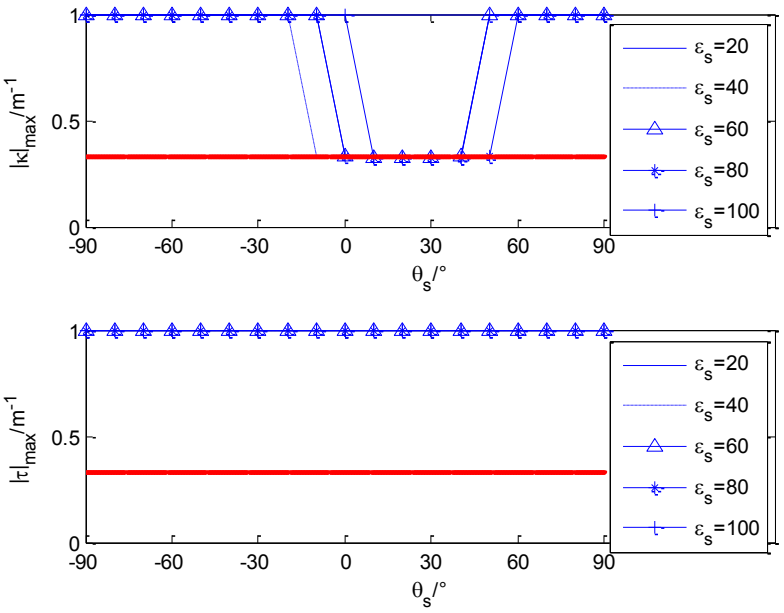

Figure 2. Path Maximum Curvature and Torsion Curve Varying with θ_s when $\varepsilon_f = 20$, ε_s Change at the Step 20

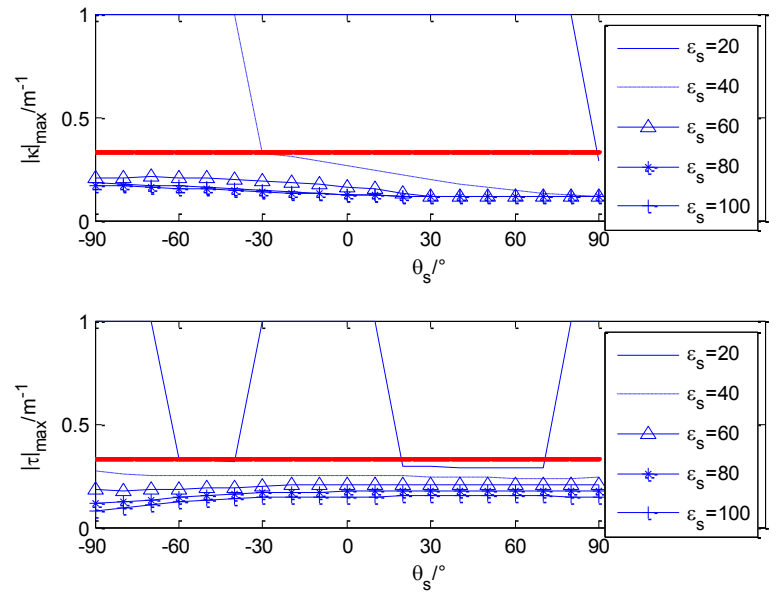

Figure 3 Path Maximum Curvature and Torsion Curve Varying with θ_s when $\varepsilon_f = 40$, ε_s Change at the Step 20

(2) Influence of the values of ε_s, ε_f on climbing angle

Under determining initial planning conditions, the relationship between climbing angle θ and ε_s, ε_f of planning path is given in Figure 5 to figure 8, among them, the horizontal coordinate is the path's length s. The tangent vector's length ε_f of ending position is 100, ε_s changes in step 100 within its scope $(400,1000)$, the biggest climbing angles of each path are shown in figure 6. The initial tangent vector's length ε_s is taken as 900, ε_f changes in step 50 within its scope $(50,350)$, the simulation results are shown in figure 7. From the figures, it can be seen that the increasing of ε_s, ε_f reduces the path's climbing angle, but the length of path will be increased.

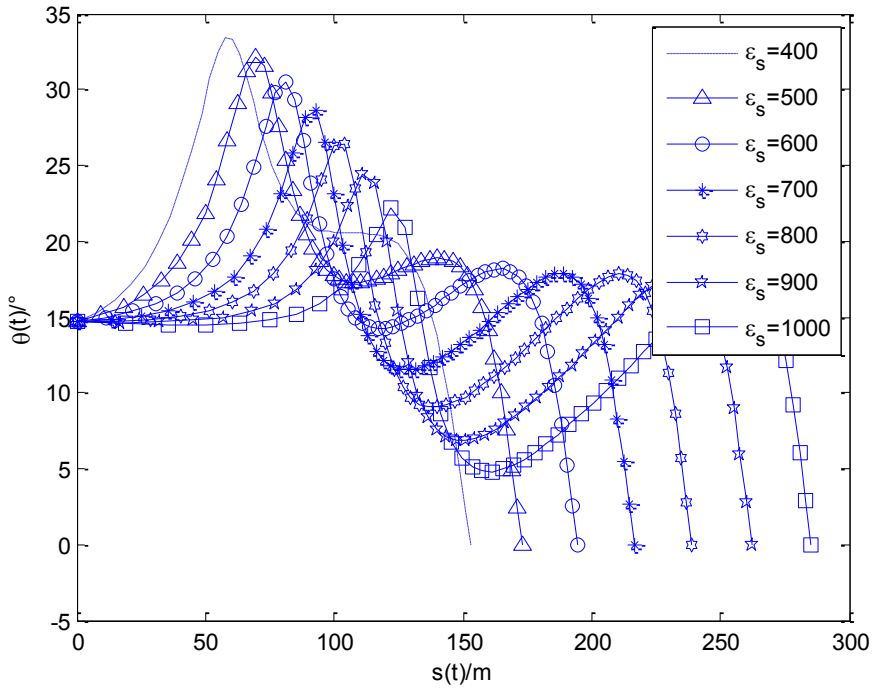

Figure 6. Path Climb Angle Curve Varying with θ_s when $\varepsilon_f = 100$, ε_s Change at the Step 100

have less number of variables. Besides, it can adopt the way of interval selection, and it is especially suitable for the situation that the feasible value ranges of ε_s , ε_f ,which meet the dynamic performance constraints, firstly need to be found out in this paper, and then do optimization. So the algorithm is proposed that Estimation of Distribution Algorithms is used to conduct optimization of path's parameters.

a. Determination on genes' value scopes

Based on the values of ε_s , ε_f , the individual genes in Estimation of Distribution Algorithms can be encoded. In order to speed up the optimization, the reasonable value ranges of each gene are given.

(1)Determination on value scopes of ε_s , ε_f that meet the constraints of torsion and curvature

Considering different initial angles and terminational angles and not considering climbing angle firstly, to analysis the maximum values of curvature and torsion under the condition that tangent vectors' length ε_s , ε_f take different values.

The shortest Dubins path's distance from the initial point to termination point can be written as $\left|p_s p_f\right|$. The tangent vectors' length are set as:

$$\varepsilon_f = \frac{1}{3}\left|p_s p_f\right| \qquad (23)$$

$$\varepsilon_s = \frac{1}{3}\left|p_s p_f\right| \qquad (24)$$

Through simulations, it found that the values of tangent vectors' angle take over the whole scope, but the curvature and torsion still can not meet the conditions ($-1/3 \le \kappa \le 1/3$, $-1/3 \le \tau \le 1/3$), the calculation results are shown in table 1.

Table 1: The Path Maximum Curvature and Torsion at Different Initial Angle with ε_s、 equal to $\frac{1}{3}\left|p_s p_f\right|$

Performance index (ϕ_s, , ,)	$\left\|\bar{\kappa}(t)\right\|_{\max}$	$\left\|\bar{\tau}(t)\right\|_{\max}$
($-\frac{\pi}{2}$, , ,)	**0.679**	**0.727**
($-\frac{\pi}{2}$, , ,)	**0.716**	**0.671**

Table 3: The Path Maximum Curvature and Torsion at Different Initial Angle with ε_s、 equal to $\frac{2}{3}\left|p_s p_f\right|$

Performance index (ϕ_s, , ,)	$\left\|\bar{\kappa}(t)\right\|_{\max}$	$\left\|\bar{\tau}(t)\right\|_{\max}$
($-\frac{\pi}{2}$, $\frac{\pi}{2}$, $\frac{\pi}{2}$)	**0.264**	**0.146**
($-\frac{\pi}{2}$, $\frac{\pi}{3}$, $\frac{\pi}{2}$)	**0.267**	**0.141**
($-\frac{\pi}{2}$, $\frac{\pi}{6}$, $\frac{\pi}{2}$)	**0.241**	**0.153**
($-\frac{\pi}{2}$, $\frac{\pi}{2}$)	**0.199**	**0.166**
($-\frac{\pi}{2}$, $\frac{\pi}{6}$, $\frac{\pi}{2}$)	**0.144**	**0.173**
($-\frac{\pi}{2}$, $\frac{\pi}{3}$, $\frac{\pi}{2}$)	**0.105**	**0.172**
($-\frac{\pi}{2}$, $\frac{\pi}{2}$, $\frac{\pi}{2}$)	**0.0927**	**0.174**

From the above analysis, the floor of ε_s , ε_f can be taken as $\frac{1}{3}\left|p_s p_f\right|$.

(2) Determination on value scopes of ε_s , ε_f that meet the constraints of climbing angle

In literature [9], the formula (5) is used to calculate the bending energy and formulas (25), (26) are adopted to do iteration of ε_s , ε_f , which make the planning path meet the constraint of climbing angle.

$$\varepsilon_s = \varepsilon_s + \left(\frac{\varepsilon_0}{\varepsilon_0 + \varepsilon_5}\right)(\rho_{\min} + \sigma_{\min}) \quad (25)$$

$$\varepsilon_f = \varepsilon_f + \left(\frac{\varepsilon_5}{\varepsilon_0 + \varepsilon_5}\right)(\rho_{\min} + \sigma_{\min}) \quad (26)$$

Among them,

$$\varepsilon_0 = \int_0^{0.5} \omega(t)^2 \left|\bar{r}(t)\right| dt$$

$$\varepsilon_5 = \int_{0.5}^{1} \omega(t)^2 \left|\bar{r}(t)\right| dt$$

IV. PATH RE-PLANNING UNDER THREATEN ENVIRONMENT

If the UAV detects obstacles in flight, the position of the insertion point and angle direction for obstacle avoidance can be calculated. The optimally flyable PH path can be generated between real-time position in which the obstacles are detected and insertion point, insertion point and termination point respectively, which are used to change the original path. In order to ensure continuity of path, the tangent direction of the path remains unchanged in detection point and insertion point.

V. SIMULATION RESULTS AND ANALYSIS OF PATH PLANNING

a. The optimization and generation of PH path

The Estimation of Distribution Algorithms, which is proposed in this paper, is used to perform simulation experiment on the three-dimensional PH path planning problem. For this simulation, the initial and final positions of the UAV, the derivatives at these positions, the kinematic constraints are summarized in table 1.

Table 1. Simulation Conditions Setting of UAV

Initial Pose			**Final Pose**			**Detection distance** (m)	**Kinematic Constraints** $\kappa_{\max}$ $\tau_{\max}$	*Climbing angle* Constraint
Position	*Derivatives*		*Position*	*Derivatives*				
	Heaing angle	*Climbing angle*		*Heading angle*	*Climbing angle*			
(0,0,0)	$-\frac{\pi}{2}$	$\frac{\pi}{12}$	(50,20,50)	$\frac{\pi}{2}$	0	100	±0.33 ±0.33	$\frac{\pi}{6}$

The selection probability of elite individual is taken as $p_e = \frac{1}{3}$ in Estimation of Distribution Algorithms. When the simulation contains climbing angle constraint, the minimum values of ε_s, ε_f can be found by the iterative method in literature [9], which satisfy three constraints. The simulation results are shown from figure 8 to figure 10. And it can get $\varepsilon_s = 942.4907$, $\varepsilon_f = 289.5093$, $|\bar{\kappa}|_{\max} = 0.233$, $|\bar{\tau}|_{\max} = 0.045$, $s = 286.1$ and the number of iterations $i = 206$.

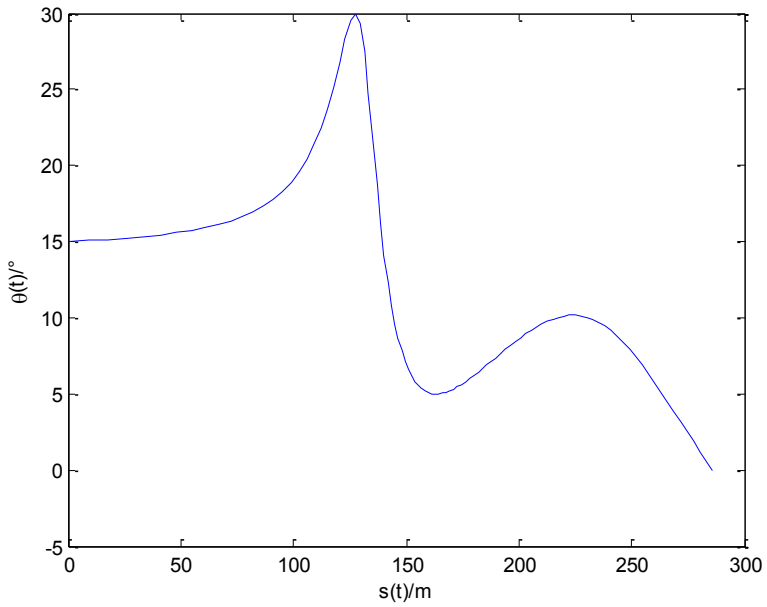

Figure 10. Climb Angle Change with the Length of the Path in Fig.8

The values of ε_s , ε_f , which are obtained by iteration, are regard as the upper limit, and $\frac{1}{3}\left|p_s p_f\right|$ is taken as the floor at the same time. The size of population is set as *N*=50, and evolutional generation is *G*=10. The parameters that correspond to the optimal value are $\varepsilon_s = 807.3519$, $\varepsilon_f = 114.7029$, $\left|\bar{\kappa}\right|_{\max} = 0.208$, $\left|\bar{\tau}\right|_{\max} = 0.234$, $\theta_{\max} = 29.2451^{\circ}$, $s = 242.0$. The parameters are set as $\lambda_1 = 0.001$, $\lambda_2 = 1$, $\lambda_3 = 1$, $\lambda_4 = 0.01$ at the time of calculating the performance index J .

When *N*=10, *G*=4, The parameters that correspond to the optimal value are $\varepsilon_s = 881.6855$, $\varepsilon_f = 197.5181$, $\left|\bar{\kappa}\right|_{\max} = 0.226$, $\left|\bar{\tau}\right|_{\max} = 0.0407$, $\theta_{\max} = 29.865^{\circ}$, $s = 245.2$. The generated path of last generation, which meets constraints, is shown in figure 11, and its curvature, torsion and climbing angle as shown in figure 12 and figure 13. The evolution curve of optimal individual's adaptive value in each generation is given in figure 14. Compared with the simulation results of *N*=50 , *G*=10, the algorithm has found a comparative optimal path, and its iteration number reduces a lot, which fully shows the rapidity of the algorithm. In comparison with the simulation results of figure 7-9, the method in this paper increase s few iterations compared with the paper [9], which can reduce the generated path's length a lot gives full consideration to the constraints of system performance.

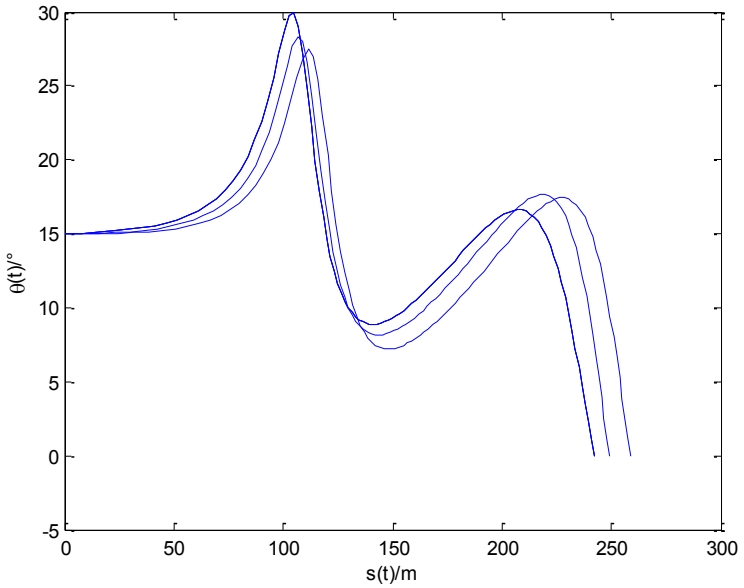

Figure 13. Climb Angle Change with the Length of the Pathes in Fig. 10

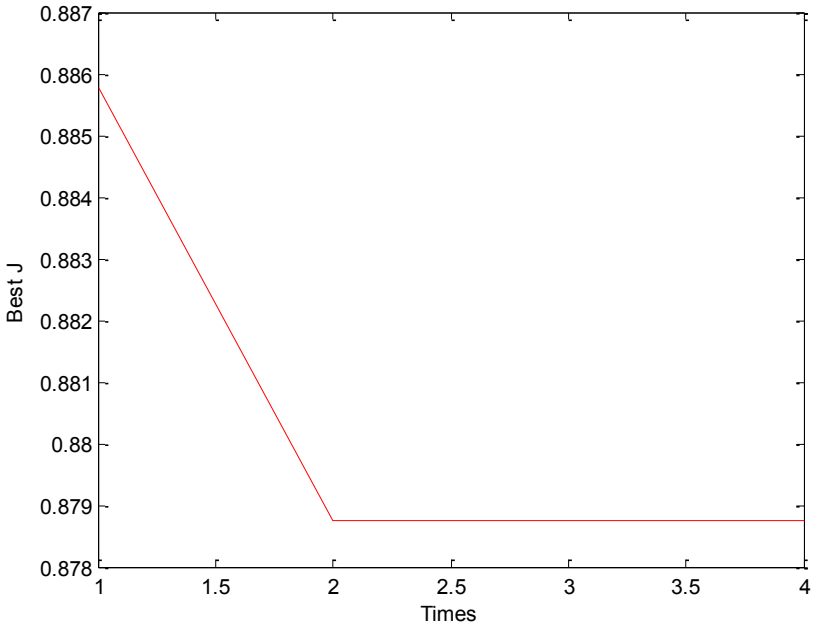

Figure 14. The Optimum Individual Fitness Evolution Curve

b. Obstacle avoidance path re-planning

For this simulation, the initial and final positions of the UAV, the derivatives at these positions, the kinematic constraints are summarized in table 2.

Table 2. Simulation Conditions Setting of UAV

Initial Pose		**Final Pose**		**Detection distance** (m)	**Kinematic Constraints**	**Velocity** (m/s)
Position	*Derivatives*	*Positio*	*Derivatives*			

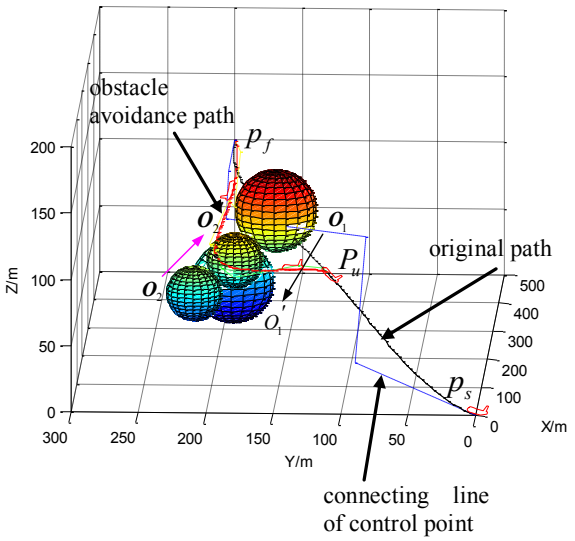

Figure 15. The Result of the obstacles Avoidance in horizontal plane

It can be seen from the simulation results that UAV successfully realize the obstacle avoidance. The horizontal or vertical plane can be selected as the plane of obstacle avoidance according to specific needs.

VI. CONCLUSION

Considering the curvature, torsion and climbing angle constraint and so on dynamic performances during UAV flights, the quantic PH curve is used to generated three dimensional path, and based on the UAV's current coordinates, speed, flight state and target point's coordinates, speed and so on information, the flyable path that is curvature continuous can be real-timely planned, which provides a kind of good practical and feasible method that can realize autonomous planning and quickly generate flyable path in the real-time dynamic environment for UAV.

VII. ACKNOWLEDGEMENTS

This research is supported by Aeronautical Science Foundation of China under Grant No20135584010.

REFERENCES

[1] Reberto Conde, David Alejo, Jose Antonio Cobano, et al. Conflict Detection and Resolution Method for Cooperationg Unmanned Aerial Vehicles[J]. J Intel Robot Syst, 2012,65: 495-505.

[2] Lugo Cardenas, I., Flores, G., Salazar, S., Lozano, R.. Dubins Path Generation for a Fixed Wing UAV[C]. 2014 International Conference on Unmanned Aircraft Systems, 2014: 339-346.

[3] R. Dai, John E. Cochran Jr. Path Planning for Multiple Unmanned Aerial Vehicles by Parameterized Corno-Spiral[C]. American Control Conference Hyatt Regency Riverfront St. Louis, MO, USA June 10-12, 2009.

[4] Ozgur Koray Sahingoz. Generation of Bezier Curve-Based Flyable Trajectories for Multi-UAV System with Paralled Genetic Algorithm[J]. Journal of Intelligent & Robotic Systems, 2014, 74(1-2):499-511.

[5] Lee Fowler1 and Jonathan Rogers , Bézier Curve Path Planning for Parafoil Terminal Guidance[C]. AIAA Aerodynamic Decelerator Systems (ADS) Conference 25-28 March 2013, Daytona Beach, Florida, AIAA 2013-1325.

[6] Armando Alves Neto, Douglas G. Macharet, Mario F. M. Campos. Feasible path planning for fixed-wing UAVs using seventh order Bézier curves[J]. Journal of the Brazilian Computer Society, 2013, 19(2):193–203.

[7] Mohammed Afzal Shah. Cooperative path planning and cooperative perception for UAVs swarm[D]. CRANFIELD UNIVERSITY. PhD Thesis, 2011.

[8] Armando A. Neto and Mario F. M. Campos. A Path Planning Algorithm for UAVs with Limited Climb Angle[C]. The 2009 IEEE/RSJ International Conference on Intelligent Robots and Systems. October 11-15, 2009 St Louis, USA:3894-3899.

[9] Armando Alves Neto, Douglas G. Macharet, Mario F. M. Campos. On the Generation of Trajectories for Multiple UAVs in Environments with Obstacles[J]. Journal of Intelligent and Robotic Systems, 2010, 57(1):123–141.

[10] Seunghan Lim, Hyochoong Bang. UAV guidance laws to arrival at desired position and time from desired direction[C]. 2011 11th International Conference on Control, Automation and Systems. Oct. 26-29, 2011 in KINTEX, Gyeonggi-do, Korea:299-304.

[11] Cheng Y H, Wang X S, Hao M L. An Estimation of distribution algorithm with diversity preservation[J]. Acta Electronica Sinica, 2010, 38(3): 591-597.

[12] F. Belkhouche and B. Bendjilali. Reactive Path Planning for 3-D Autonomous Vehicles[J]. IEEE Transactions on Control Systems Technology. Vol. 20, No. 1, JANUARY 2012.

[13] D. Alejo, J.A.Cobano, M.A.Trujillo, et al. The Speed Assignment Problem for Conflict Resolution In Aerial Robotics[C]. 2012 IEEE International Conference on Robotics and Automation, May 14-18,2012: 3919-3424.

[14] T. Lauderdale, Probabilistic conflict detection for robust detection and resolution[C]. Proc. AIAA Aviation Technol., Integr., Oper., Indianapolis, 2012: 1–12.

[15] Basheer, G.S.,Ahmad, M.S.,Tang, A.Y.C.: A Framework for Conflict Resolution in Multi-agent Systems[C]. ICCCI2013. LNCS, Springer, vol.8083, 2013:195-204

[16] Ghusoon Salim Basheer1, Mohd Sharifuddin Ahmad1, Alicia Y.C. Tang1, et.al. A Novel Conflict Resolution Strategy in Multi-agent Systems: Concept and Model[C]. Advanced Approaches to Intelligent Information and Database Systems, Studies in Computational Intelligence 551, 2014: 35-45